Generation of Recombinant Rotavirus Expressing NSP3-UnaG Fusion Protein by a Simplified Reverse Genetics System

Asha A. Philip[a], Heather E. Eaton[b], Maya Shmulevitz[b], and John T. Patton[a#]

[a]Department of Biology, Indiana University, Bloomington, Indiana, USA

[b]Department of Medical Microbiology and Immunology, University of Alberta, Edmonton, Alberta, Canada

#Corresponding address: John T. Patton, Department of Biology, Indiana University, 212 S. Hawthorne Drive, Simon Hall 011, Bloomington, IN 47405 USA

Running title: Rotavirus Encoding NSP3-Fluorescent Protein

Email addresses:

Asha A. Philip, aaphilip@iu.edu; Heather E. Heaton, heeaton@ualberta.ca; Maya Shmulevitz, shmulevi@ualberta.ca; John T. Patton. jtpatton@iu.edu

18 **Abstract**

19 Rotavirus is a segmented double-stranded (ds)RNA virus that causes severe gastroenteritis in
20 young children. We have established an efficient simplified rotavirus reverse genetics (RG)
21 system that uses eleven T7 plasmids, each expressing a unique simian SA11 (+)RNA, and a
22 CMV support plasmid for the African swine fever virus NP868R capping enzyme. With the
23 NP868R-based system, we generated recombinant rotavirus (rSA11/NSP3-FL-UnaG) with a
24 genetically modified 1.5-kB segment 7 dsRNA that encodes full-length NSP3 fused to UnaG, a
25 139-aa green fluorescent protein (FP). Analysis of rSA11/NSP3-FL-UnaG showed that the virus
26 replicated efficiently and was genetically stable. The NSP3-UnaG fusion product was well
27 expressed in rSA11/NSP3-FL-UnaG-infected cells, reaching levels similar to NSP3 in wildtype
28 rSA11-infected cells. Moreover, the NSP3-UnaG protein, like functional wildtype NSP3, formed
29 dimers *in vivo*. Notably, NSP3-UnaG protein was readily detected in infected cells via live cell
30 imaging, with intensity levels much greater than that of the NSP1-UnaG fusion product of
31 rSA11/NSP1-FL-UnaG. Our results indicate that FP-expressing recombinant rotaviruses can be
32 made through manipulation of the segment 7 dsRNA without deleting or interrupting any of the
33 twelve open reading frames of the virus. Because NSP3 is expressed at levels higher than NSP1
34 in infected cells, rotaviruses expressing NSP3-based FPs may be a more sensitive tool for
35 studying rotavirus biology than rotaviruses expressing NSP1-based FPs. This is the first report of
36 a recombinant rotavirus containing a genetically engineered segment 7 dsRNA.

37

38 **Importance**

39 Previous studies have generated recombinant rotaviruses that express fluorescent proteins (FPs)
40 by inserting reporter genes into the NSP1 open reading frame (ORF) of genome segment 5.

Unfortunately, NSP1 is expressed at low levels in infected cells, making viruses expressing FP-fused NSP1 less than ideal probes of rotavirus biology. Moreover, FPs were inserted into segment 5 in such a way as to compromise NSP1, an interferon antagonist affecting viral growth and pathogenesis. We have identified an alternative approach for generating rotaviruses expressing FPs, one relying on fusing the reporter gene to the NSP3 ORF of genome segment 7. This was accomplished without interrupting any of the viral ORFs, yielding recombinant viruses likely expressing the complete set of functional viral proteins. Given that NSP3 is made at moderate levels in infected cells, rotavirus encoding NSP3-based FPs should be more sensitive probes of viral infection than rotaviruses encoding NSP1-based FPs.

Key words (3-6)

rotavirus, reverse genetics, green fluorescent protein, African swine fever virus capping enzyme

54

55 **Introduction**

56 Group A rotavirus (RVA) is a primary cause of acute gastroenteritis in infants and
57 children under 5 years of age (Crawford et al., 2017). The RVA genome consists of eleven
58 segments of double-stranded (ds)RNA, with a total size of ~18 kB, and is contained within a
59 non-enveloped icosahedral capsid composed of three concentric protein layers (Settembre et al.,
60 2011). During replication, the genome segments are transcribed, producing eleven 5'-capped, but
61 non-polyadenylated (+)RNAs (Imai et al., 1983; Trask et al., 2012). The (+)RNAs are generally
62 monocistronic, each with a single open reading frame (ORF) that specifies one of the six
63 structural (VP1-VP4, VP6-VP7) or six nonstructural (NSP1-NSP6) proteins of the virus. The
64 (+)RNAs also serve as templates for the synthesis of dsRNA genome segments (Gugliemli et al.,
65 2010).

66 Insights into RVA biology have been severely hampered by the lack of a reverse genetics
67 (RG) system to unravel details into the replication and pathogenesis mechanisms of the virus.
68 This limitation was recently overcome by Kanai et al. (2017), who described the development of
69 a fully plasmid-based RG system that allowed genetic engineering of the prototypic RVA simian
70 SA11 strain. Key to the RG system was co-transfection of baby hamster kidney cells expressing
71 T7 RNA polymerase (BHK-T7 cells) with T7 plasmids directing synthesis of the eleven SA11
72 (+)RNAs, two CMV plasmids encoding the vaccinia virus D1L-D12R capping enzyme complex
73 (Kyrieleis et al., 2014), and another CMV plasmid encoding the avian reovirus p10FAST fusion
74 protein (Salsman et al., 2005). Subsequent publications described changes to the Kanai RG
75 system designed to reduce its complexity and/or enhance the recovery of recombinant virus.
76 Notably, Komoto et al (2018) showed that recombinant virus could be produced simply by

77 transfecting BHK-T7 cells with eleven SA11 T7 plasmids, with the caveat that plasmids for the
78 viroplasm building blocks (NSP2 and NSP5) (Fabbretti et al., 1999; Eichwald et al., 2004) be
79 added at levels three-fold greater than the other plasmids. Of possible significance, the Komoto
80 RG system used a set of SA11 T7 plasmids with vector backbones that differed in size and
81 sequence from the SA11 T7 plasmids described by Kanai et al (2017).

82 Plasmid-based RG systems have been used to modify several SA11 genome segments,
83 with the focus mostly on segment 5, which encodes NSP1 (Kanai et al., 2017, 2018; Komoto et
84 al., 2018). Through insertion of reporter genes into the segment 5 dsRNA, recombinant RVAs
85 have been produced that express fluorescent reporter proteins (FPs) (e.g., mCherry, eGFP)
86 (Kanai et al., 2017, 2018; Komoto et al., 2018); these FP-RVAs are important tools for studying
87 virus replication and pathogenesis via live cell imaging and other fluorescence-based approaches.
88 Unfortunately, the segment 5 product NSP1 is expressed at low levels in infected cells and is
89 subject to proteasomal degradation making FP-fused NSP1 proteins less than ideal probes of
90 RVA biology (Martinez-Alvarez et al., 2013). Moreover, FP genes were inserted into the
91 segment 5 dsRNA in such a way as to alter the NSP1 open reading frame (ORF), likely
92 compromising the protein's function as an IFN-antagonist (Barro and Patton, 2005; Davis and
93 Patton, 2017) and, thus, impacting the virus's biological properties.

94 In this study, we explored an alternative approach for making FP-RVAs, one relying on
95 modification of the genome segment that expresses NSP3 (segment 7), a viral translation
96 enhancer expressed at moderate levels in the infected cell that may not be required for virus
97 replication (Montero et al., 2006; Gratia et al., 2015). In generating recombinant RVAs, we
98 employed a simplified RG system requiring only a single support plasmid: a CMV expression
99 vector for the African swine fever virus (ASFV) NP868R capping enzyme (Dixon et al., 2013).

100 Using the NP868R-based RG system, we produced a novel SA11 strain with modified segment 7
101 dsRNA that expressed NSP3 fused to the green fluorescent protein (FP) UnaG. This is the first
102 RVA strain engineered to produce a FP that did not involve deleting or interrupting any of one of
103 the 12 viral ORFs, thus yielding a recombinant virus likely expressing a complete set of
104 functional viral proteins.
105

106 **Materials and methods**

107 *Cell culture.* Embryonic monkey kidney cells (MA104) were grown in M199 complete
108 medium [Medium 199 (Lonza) and 1% penicillin-streptomycin (P/S) (Corning)] containing 5%
109 fetal bovine serum (FBS) (Gibco) (Arnold et al., 2009). BHK-T7 cells were a kind gift from Drs.
110 Ulla Buchholz and Peter Collins, Laboratory of Infectious Diseases, NIAID, NIH. BHK-T7 cells
111 were grown in Glasgow complete medium [Glasgow minimum essential medium (G-MEM)
112 (Lonza), 10% tryptone-peptide broth (Gibco), 1% P/S, 2% non-essential amino acids (NEAA)
113 (Gibco), and 1% glutamine (Gibco)] containing 5% heat-inactivated FBS. Medium used to
114 cultivate BHK-T7 cells was supplemented with 2% G418 geneticin (Invitrogen) every other
115 passage.

116 *Plasmid construction.* RVA (simian SA11 strain) plasmids pT7/VP1SA11,
117 pT7/VP2SA11, pT7/VP3SA11, pT7/VP4SA11, pT7/VP6SA11, pT7/VP7SA11, pT7/NSP1SA11,
118 pT7/NSP2SA11, pT7/NSP3SA11, pT7/NSP4SA11, and pT7/NSP5SA11 were kindly provided
119 by Dr. Takeshi Kobyashi (Kanai et al., 2017) through the Addgene plasmid repository
120 {https://www.addgene.org/Takeshi_Kobayashi/}. To generate the pCMV/NP868R plasmid, a
121 DNA representing the ASFV NP868R ORF (Genbank NP_042794), bound by upstream *Xba*I
122 and downstream *Bam*HI sites, was synthesized by Genscript and inserted into the *Eco*RV site of

123 the pUC57 plasmid. A DNA fragment containing the NP868R ORF was recovered from the
124 plasmid by digestion with *Not*I and *Pvu*I and ligated into the plasmid pCMV-Script (Agilent
125 Technologies), cut with the same two restriction enzymes. pT7/NSP3-FL-UnaG was constructed
126 by fusing a DNA fragment containing the ORF for 3xFL-UnaG to the 3'-end of the NSP3 ORF in
127 pT7/NSP3SA11 using a Takara In-fusion HD cloning kit. The 3xFL-UnaG fragment was
128 amplified from the reovirus S1 3xFL-UnaG plasmid (Eaton et al, 2017) using the primer pair 5'-
129 tcatttggttgcgaagactacaaagaccatgacggtgattataaaga-3'
130 and 5'-catgtatcaaaatggtcattctgtggcccttctgtagct-3' and the pT7/NSP3SA11 plasmid was amplified
131 using the NSP3 primer pair 5'-ccattttgatacatgttgaacaatcaaatacagtgt-3' and 5'-
132 ttcgcaaccaaatgaatattgataattacatctctgtattaat-3'. pT7/NSP1-FL-UnaG was constructed by inserting
133 the 3xFL-UnaG fragment into the NSP1 ORF of the segment 5 cDNA (position 1199) in
134 pT7/NSP1SA11. For cloning, the pT7/NSP1SA11 plasmid was amplified using the NSP1 primer
135 pair 5'- tgaagaagtgtttaatcacatgtcgcc-3' and 5'- tttgatccatgtgattagtaaacaaactccaaa-3 and the 3xFL-
136 UnaG insert was amplified from pT7/NSP3-R2A-FL-UnaG using the primer pair 5'-
137 tcacatggatcaaacctacaaagaccatgacggtgattataaagatcat-3' and 5'-
138 ttaaacacttcttcatcattctgtggcccttctgtagc-3'. Transfection quality plasmids were prepared
139 commercially (www.plasmid.com) or using a QIAprep spin miniprep kit. Primers were provided
140 by Integrated DNA Technologies (IDT) and plasmid sequences were determined by ACGT.
141 Sequences of recombinant RVAs were determined from cDNAs prepared from viral RNAs using
142 a Superscript III reverse transcriptase kit (Invitrogen).
143 *Optimized RVA RG protocol.* On Day 0, freshly confluent monolayers of BHK-T7 cells
144 were disrupted using trypsin-versine and resuspended in G418-free Glasgow complete medium
145 containing 5% FBS. Cell numbers were determined with a Nexcelom Cellometer AutoT4

146 counter. The cells were seeded in the same medium into 12-well plates (2-4 x 10^5 cells/well). On
147 Day 1, plasmid mixtures were prepared that contained 0.8 μg each of the 11 RVA pT7 plasmids,
148 except pT7/NSP2SA11 and pT7/NSP5SA11, which were 2.4 μg each. Included in plasmid
149 mixtures was 0.8 μg of pCMV/NP868R. The plasmid mixtures were added to 100 μl of pre-
150 warmed (37°C) Opti-MEM (Gibco) and mixed by gently pipetting up and down. Afterwards, 25
151 μl of TransIT-LTI transfection reagent (Mirus) was added, and the transfection mixtures gently
152 vortexed and incubated at room temperature for 20 min. During the incubation period, BHK-T7
153 cells in 12-well plates were washed once with Glasgow complete medium, and then 1 ml of
154 SMEM complete medium [MEM Eagle Joklik (Lonza), 10% TBP, 2% NEAA, 1% P/S, and 1%
155 glutamine)] was placed in each well. The transfection mixture was added drop-by-drop to the
156 medium in the wells and the plates returned to a 37°C incubator. On Day 3, 2 x10^5 MA104 cells
157 in 250 μl of M199 complete medium were added to wells, along with trypsin to a final
158 concentration of 0.5 μg/ml (porcine pancreatic type IX, Sigma Aldrich). On Day 5, cells in plates
159 were freeze-thawed 3-times and the lysates placed in 1.5 ml microfuge tubes. After
160 centrifugation at 500 x g for 10 min (4°C), 300 μl of the supernatant was transferred onto
161 MA104 monolayers in 6-well plates containing 2 ml of M199 complete medium and 0.5 μg/ml
162 trypsin. The plates were incubated at 37°C for 7 days or until complete cytopathic effects (CPE)
163 were observed. Typically, complete CPE was noted at 4-6 days p.i. for wells containing
164 replicating RVA.

165 *Analysis of recombinant viruses.* RVAs were propagated in MA104 cells in M199
166 complete medium containing 0.5 μg/ml trypsin. Viruses were isolated and titered by plaque
167 assay on MA104 cells (Arnold et al., 2009). Viral RNAs were recovered from clarified infected-
168 cell lysates by Trizol extraction, resolved by electrophoresis on Novex 8% polyacrylamide gels

169 (Invitrogen), and detected by staining with ethidium bromide. Live cell imaging was performed
170 on MA104 cells infected at a multiplicity of infection (MOI) of 3 using a Bio-Rad Zoe
171 fluorescence imager.

172 For immunoblot assays, proteins in lysates prepared at 8 h p.i. from MA104 cells infected
173 with RVA at an MOI of 5 were resolved by electrophoresis on Novex linear 8-16%
174 polyacrylamide gels and transferred to nitrocellulose membranes. After blocking with phosphate-
175 buffered saline containing 5% nonfat dry milk, blots were probed with guinea pig polyclonal
176 NSP3 (Lot 55068, 1:2000) or VP6 (Lot 53963, 1:2000) antisera (Arnold et al., 2012), or mouse
177 monoclonal Flag M2 (Sigma F1804, 1:2000) or rabbit monoclonal PCNA (13110S, Cell
178 Signaling Technology (CST), 1:1000) antibody. Primary antibodies were detected using
179 1:10,000 dilutions of horseradish peroxidase (HRP)-conjugated secondary antibodies: horse anti-
180 mouse IgG (CST), anti-guinea pig IgG (KPL), or goat anti-rabbit IgG (CST). Signals were
181 developed using Clarity Western ECL Substrate (Bio-Rad) and detected using a Bio-Rad
182 ChemiDoc imaging system. Image J analysis was used to determine the intensity of bonds on
183 immunoblots {https://imagej.net/ImageJ}.

184 To assess genetic stability, MA104 cells were infected with recombinant RVA at an MOI
185 of ~0.1. When cytopathic effects were complete (4-5 days p.i.), the cells were freeze-thawed
186 twice in their medium, and lysates were centrifuged at low speed to remove debris. Virus in
187 clarified lysates was serially passaged 5 times, infecting MA104 cells with 2 μl of lysate
188 combined with 2 ml of fresh M199 complete medium. Double-stranded RNA in clarified lysates
189 was examined by gel electrophoresis and detected by staining with ethidium bormide.

190 *Nucleotide sequence accession numbers.* pCMV/NP868R, MH212166; pT7/NSP3-FL-
191 UnaG, MK868472; and, pT7/NSP1-FL-UnaG, MH197081.

192

193 **Results and Discussion**

194 *NP868R-based RG system*. A previous study showed that addition of a CMV plasmid
195 expressing the ASFV NP868R capping enzyme to the mammalian reovirus RG system
196 significantly increased recovery of recombinant virus (Eaton et al., 2017). Based on this finding,
197 we constructed a similar CMV plasmid for NP868R (pCMV/NP868R) and evaluated whether its
198 co-transfection with SA11 pT7 plasmids into BHK-T7 cells was sufficient to allow recovery of
199 recombinant RVAs. In our RG experiments, two different types of pT7 vectors for segment 7
200 (NSP3) were used, one (pT7/NSP3SA11) designed to introduce a wild type segment 7 dsRNA
201 into recombinant RVA and the second (pT7/NSP3-FL-UnaG) designed to test the possibility of
202 introducing a modified segment 7 RNA that expressed NSP3 with a fluorescent tag. To construct
203 pT7/NSP3-FL-UnaG, the C-terminus of the NSP3 ORF in pT7/NSP3SA11 was fused to the ORF
204 for UnaG, a 139-amino acid (aa) green fluorescent protein of the Unagi eel that utilizes bilirubin
205 as a fluorophore (Kumagai et al., 2013) (Fig. 1). To further ease detection of the protein product
206 of the modified pT7 plasmid, a 3x Flag sequence was inserted between the NSP3 ORF and UnaG
207 ORF. As a result of the addition of Flag and UnaG sequences, the pT7/NSP3-FL-UnaG vector
208 expresses a 1.6-kb RNA that encodes a 477-aa protein instead of the 1.1-kb RNA and 315-aa
209 protein of pT7/NSP3SA11 (Fig. 1). The NSP3-FL-UnaG fusion protein retained the same RNA-
210 binding domain, coiled-coil dimerization domain, and eIF4G-binding domain present in wildtype
211 NSP3 (Deo et al., 2002; Groft et al., 2002).

212 Rotavirus RG experiments were performed using stocks of BHK-T7 cells maintained in
213 Glasgow medium enriched with FBS, tryptone-peptide broth, and non-essential amino acids.
214 Mixtures of RG plasmids were transfected into BHK-T7 cells that were ~90% confluent and had

215 been seeded into 12-well plates the day before. In our optimized protocol, plasmid mixtures
216 included pCMV/NP868R, 3x levels of pT7/NSP2SA11 and pT7/NSP5SA11, either
217 pT7/NSP3SA11 or pT7/NSP3-FL-UnaG, and the remaining SA11 pT7 plasmids. Transfected
218 BHK-T7 cells were over seeded with MA104 cells to promote amplification of recombinant
219 viruses. At 5 days post transfection, the cells were freeze-thawed thrice and large debris removed
220 by low speed centrifugation. Recombinant viruses in cell lysates were amplified by passage in
221 MA104 cells, plaque isolated, and amplified again in MA104 cells.
222 *Recombinant RVA expressing fused NSP3-UnaG*. Analysis of the cell lysates showed that
223 transfection of BHK-T7 cells with RG plasmid mixtures using the optimized protocol supported
224 the generation of recombinant RVAs, including SA11 isolates with a wildtype segment 7 (NSP3)
225 dsRNA (rSA11/wt) or a modified segment 7 RNA (rSA11/NSP3-FL-UnaG) (Fig. 2). RG
226 experiments performed with this plasmid mixture (pCMV/NP868R plus 3x each pT7/NSP2SA11
227 and pT7/NSP5/SA11) generated more recombinant RVA than RG experiments performed with
228 plasmid mixtures that contained just pCMV/NP868R or 3x each pT7/NSP2SA11 and
229 pT7/NSP5SA11 (Fig. S1). The identity of the modified segment 7 dsRNA in rSA11/NSP3-FL-
230 UnaG was verified by gel electrophoresis (Fig. 2A), which revealed that the wildtype 1-kB
231 segment 7 dsRNA had been replaced with a segment co-migrating with the 1.5-kB segment 5
232 (NSP1) dsRNA. The authenticity of the segment 7 dsRNA in rSA11/NSP3-FL-UnaG was
233 confirmed by RT-PCR and sequencing (data not shown). Immunoblot analysis with anti-NSP3
234 and anti-FLAG antibodies of infected cell lysates indicated that segment 7 of rSA11/NSP3-FL-
235 UnaG expressed a protein of the expected size (55 kD) for NSP3-FL-UnaG and did not express
236 the wildtype 37-kD NSP3 (Fig. 2B). As a probe of the properties of NSP3-FL-UnaG, we
237 examined whether the protein was able to form dimers in infected cells, as previously reported

238 for wildtype NSP3 (Arnold, 2013). Indeed, electrophoretic analysis of rSA11/NSP3-UnaG-
239 infected cell lysates treated with denaturing sample buffer at 25ºC showed that the NSP3-FL-
240 UnaG migrated as a dimer (Fig. 3), suggesting that the NSP3 coiled-coil dimerization domain
241 retains its function in the fusion product. Under these same electrophoretic conditions, the VP6
242 inner capsid protein of both rSA11/NSP3-FL-UnaG and rSA11/wt formed trimers that were
243 stable at 25ºC (Fig. 3) (Clapp and Patton, 1991). Quantitation of bands appearing on
244 immunoblots probed with anti-NSP3 and anti-VP6 antibodies indicated that the steady-state level
245 of NSP3-FL-UnaG (normalized to VP6) in rRVA/NSP3-FL-UnaG-infected cells approximated
246 that of the steady-state level of NSP3 in rRVA/wt infected cells (Fig. 3, lanes 4 versus 6). Thus,
247 the segment 7 (+)RNAs of rRVA/NSP3-FL-UnaG and rRVA/wt appear to be translated with
248 near equal efficiency.

249 Plaque analysis showed that rSA11/wt and rSA11/NSP3-FL-UnaG grew to similar peak
250 titers (~1.25 x 10^7 and ~7.5 x 10^6, respectively) and generated plaques of similar size on MA104
251 cells (Fig. 2C). Five-rounds of serial passage of rSA11/NSP3-FL-UnaG at low MOI revealed no
252 difference in the dsRNA profile of the starting virus and passage 5 virus, indicating that the
253 recombinant RVA was genetically stable (Fig. 4).

254 *Fluorescence signal of rSA11/NSP3-FL-UnaG*. Examination of MA104 cells infected
255 with rSA11/NSP3-FL-UnaG by live-cell fluorescent imager confirmed that UnaG was
256 functional, emitting fluorescent light in a range overlapping green fluorescent protein (GFP)
257 (Fig. 5) (Rodriguez et al., 2017). The signal predominantly localized to the cytoplasm, where it
258 was distributed in a punctate like manner, reminiscent of previous reports analyzing the
259 distribution of NSP3 in infected cells by immunofluorescence using anti-NSP3 antibody (Rubio
260 et al., 2013). To contrast the intensity of the fluorescent signal produced by recombinant viruses

261 expressing UnaG fused to NSP3 versus NSP1, we generated rSA11/NSP1-FL-UnaG (Fig. 6)
262 using the optimized NP868R-based RG protocol. To produce this virus, a FL-UnaG ORF
263 terminating with a stop codon was inserted into NSP1 ORF of the segment 5 cDNA of
264 pT7/NSP1SA11. As illustrated in Fig. 6, pT7/NSP1-FL-UnaG produces a 2.1-kb RNA that
265 encodes a 575-aa protein instead of the 1.6-kb RNA and 520-aa protein of pT7/NSP1SA11. The
266 segment-5 protein product of pT7/NSP1-FL-UnaG ends with the same Flag-UnaG cassette as the
267 segment-7 protein product of pT7/NSP3-FL-UnaG.

268 As determined by gel electrophoresis (Fig. 6) and sequencing (not shown), the genome of
269 rSA11/NSP1-FL-UnaG included the expected large 2.1-kB segment 5 dsRNA. Immunoblot
270 analysis of rSA11/NSP1-FL-UnaG-infected cell lysates using anti-Flag antibody indicated that
271 the virus also encoded the NSP1-FL-UnaG product. Based on plaque assay, rSA11/NSP1-FL-
272 UnaG grew to a peak titer (~4.5 x10^7) exceeding that of rSA11/wt by approximately 2-fold.
273 rSA11/NSP1-FL-UnaG has a plaque size slightly smaller than wildtype virus (Fig. 6), a
274 phenotype noted before for RVAs encoding truncated or altered NSP1 proteins (Patton et al.,
275 2001).

276 Live-cell imagining revealed that the intensity of UnaG fluorescence signal was markedly
277 greater in MA104 cells infected with rSA11/NSP3-FL-UnaG than rSA11/NSP1-FL-UnaG (Fig.
278 5). This result suggests that RVAs expressing fused NSP3-FPs may be more sensitive probes of
279 viral infection that RVAs expressing fused NSP1-FPs.

280 *Stem-loop structure in the segment 7 3'-UTR*. rSA11/NSP3-FL-UnaG was generated by
281 placing a nonviral 500-bp insert into the segment 7 dsRNA at the junction of the NSP3 ORF and
282 3'-UTR. Similar recombinant RVAs have been made by inserting nonviral sequences between
283 the NSP2 ORF and 3'-UTR of the segment 8 dsRNA (Navarro et al., 2013). Thus, the junction

284 between the viral ORF and 3'-UTR may represent a site well suited for the introduction of long
285 foreign sequences into RVA genome segments. Interestingly, for RVAs with naturally occurring
286 genome rearrangements, this is the same site in segment 5, 6, 7, 10 and 11 dsRNAs in which
287 viral sequence duplications have been noted to initiate (Ballard et al., 1992; Shen et al., 1994;
288 Gault et al., 2001; Patton et al., 2001; Arnold et al., 2012). The 3'-UTR contains multiple *cis*-
289 acting signals important to rotavirus replication, including sequences that are recognized by the
290 RVA RNA polymerase VP1 and the translation enhancer NSP3 (Deo et al., 2002; Tortorici et al.,
291 2003). The fact that well-growing genetically-stable recombinant RVAs have been recovered in
292 which a viral ORF has been separated from its 3'-UTR indicates that *cis*-acting signals in the 3'-
293 UTR continue to function even though displaced linearly a long distance from the remaining
294 viral sequence of the RNA.

295 In a previous study (Navarro et al., 2013), an *in silico* RNA folding analysis
296 {*http://rna.tbi.univie.ac.at/cgi-bin/RNAfold.cgi*} was performed to probe how the insertion of
297 sequence duplications and foreign sequences effected the predicted secondary structure of the
298 mutant segment 8 (+)RNAs used in making recombinant RVAs. The results showed that despite
299 extensive differences in the overall folding predictions of the mutant RNAs, in all cases their 5'-
300 and 3'-UTRs interacted to form stable 5'-3' panhandles. In addition, the predictions all revealed
301 an identical stem-loop structure projecting from the 5' side of the 5'-3 panhandle, formed by
302 residues that are highly conserved among RVA segment 8 RNAs. The conservation of the
303 structure and its sequence suggested that the stem-loop may function as a segment specific
304 packaging signal (Navarro et al., 2013). We performed a similar *in silico* RNA folding analysis,
305 contrasting the secondary structures predicted for the segment 7 RNAs of rSA11/wt and
306 rSA11/NSP3-FL-UnaG. The results showed that the overall secondary structures predicted for

307 the RNAs differed considerably, with the notable exception that extending from the 3'-UTR of
308 both RNAs was a long (~70 base) stable stem-loop structure formed by sequences that are highly
309 conserved in RVA segment 7 RNAs (Fig. 7). The stability and location of the stem-loop suggests
310 that this structure may function as a segment specific packaging signal, in a manner previously
311 proposed for the conserved stem-loop detected in the segment 8 RNA.

312 *Summary*. rSA11/NSP3-FL-UnaG is the first recombinant RVA to be described with a
313 modified segment 7 dsRNA. Segment 7 joins segments 4 (VP4) (Johne et al., 2015; Mohanty et
314 al., 2017), 5 (NSP1) (Kanai et al., 2019), 8 (NSP2) (Trask et al., 2010; Navarro et al., 2013), and
315 11 (NSP5/NSP6) (Komoto et al., 2017) as targets altered by RG and represents only the second
316 RVA segment to be used as a vector for FP expression. Our analysis of rSA11/NSP3-FL-UnaG
317 indicates that it is possible to generate recombinant RVAs that express FPs through their fusion
318 to the C-terminus of NSP3. Given that NSP3 is expressed at moderate levels in infected cells,
319 RVAs expressing NSP3-based FPs may be more effective indicators of viral replication in live
320 cell imagining experiments and other fluorescence-based assay systems than RVAs expressing
321 NSP1-based FPs, since NSP1 is expressed at low levels *in vivo* (Martinez-Alvarez et al., 2013).
322 Although several recombinant RVAs that express FPs have been described, rSA11/NSP3-FL-
323 UnaG is unique among them in that none of its ORFs have been deleted or interrupted. Instead,
324 the only impact on rSA11/NSP3-FL-UnaG was to fuse its NSP3 ORF to a FL-UnaG ORF.
325 Importantly, although the NSP3 ORF in RVA strains is not naturally extended and does not
326 encode NSP3 fused to a downstream protein, the NSP3 ORF of group C rotaviruses (RVCs) is
327 extended, encoding an NSP3 protein that is fused to a 2A stop-start translational element
328 (Donnelly et al., 2001) and double-stranded RNA binding protein (dsRBP) (James et al., 1999;
329 Langland et al., 1994). Given that RVC segment 6 encodes an NSP3 fusion protein, it seems

330 likely that the NSP3 fusion protein of rSA11/NSP3-FL-UnaG remains functional, even when
331 fused to a downstream protein. Interestingly, despite repeated attempts, we were unsuccessful in
332 generating recombinant RVAs using mutated pT7/NSP3SA11 plasmids in which the NSP3 ORF
333 was interrupted through insertion of stop codons (data not shown). This result implies that NSP3
334 is essential for RVA replication or is required to generate recombinant viruses using the RG
335 system.

336 Our results suggest that the RVA segment 7 RNA can be re-engineered to function as an
337 expression vector of foreign proteins, without compromising the function of any of the viral
338 ORFs. It remains unclear how much foreign sequence can be inserted into the segment 7 RNA,
339 but our analysis so-far indicates that it is possible to generate well replicating viruses carrying
340 >500 bp of extra sequence. Given the remarkable flexibility so far noted in the ability of the
341 rotavirus to accommodate changes in the size and sequences of its RNA, the virus may turn out
342 to be particularly empowering tool for unraveling the shared mechanisms used by the *Reoviridae*
343 to package and replicate their genomes.

344

345 **Acknowledgments.** We are grateful to all the members of the Patton and Danthi laboratory for
346 their support and encouragement on this project. Our thanks also go to Ulla Buckholtz and Peter
347 Collins, NIAID, NIH for their gift of BHK-T7 cells. This work was supported by National
348 Institutes of Health grants R03 AI131072 and R21 AI144881, Indiana University Start-Up
349 Funding, and the Lawrence M. Blatt Endowment.

350 **References**

351 1. Arnold, M., Patton, J.T., McDonald, S.M. 2009. Culturing, storage, and quantification of
352 rotaviruses. Curr Protoc Microbiol Chapter 15:Unit 15C.3.
353 2. Arnold, M.M., Brownback, C.S., Taraporewala, Z.F., Patton, J.T. 2012. Rotavirus variant
354 replicates efficiently although encoding an aberrant NSP3 that fails to induce nuclear
355 localization of poly(A)-binding protein. J. Gen. Virol. 93:1483-1494.
356 3. Ballard, A., McCrae, M.A., Desselberger, U. 1992. Nucleotide sequences of normal and
357 rearranged RNA segments 10 of human rotaviruses. J. Gen. Virol. 73:633-638.
358 4. Barro, M., Patton, J.T. 2005. Rotavirus nonstructural protein 1 subverts innate immune
359 response by inducing degradation of IFN regulatory factor 3. Proc. Natl. Acad. Sci. USA
360 102:4114-4119.
361 5. Clapp, L.L., Patton, J.T. 1991. Rotavirus morphogenesis: domains in the major inner capsid
362 protein essential for binding to single-shelled particles and for trimerization. Virology
363 180:697-708.
364 6. Crawford, S.E., Ramani, S., Tate, J.E., Parashar, U.D., Svensson, L., Hagbom, M., Franco,
365 M.A., Greenberg, H.B., O'Ryan, M., Kang, G., Desselberger, U., Estes, M.K. 2017.
366 Rotavirus infection. Nat. Rev. Dis. Primers 3:17083.
367 7. Davis, K.A., Patton, J.T. 2017. Shutdown of interferon signaling by a viral-hijacked E3
368 ubiquitin ligase. Microb. Cell. 4:387-389.
369 8. Deo, R.C., Groft, C.M., Rajashankar, K.R., Burley, S.K. 2002. Recognition of the rotavirus
370 mRNA 3' consensus by an asymmetric NSP3 homodimer. Cell 108:71-81.
371 9. Dixon, L.K., Chapman, D.A., Netherton, C.L., Upton, C. 2013. African swine fever virus
372 replication and genomics. Virus Res. 173:3-14.

373 10. Donnelly, M.L., Hughes, L.E., Luke, G., Mendoza, H., ten Dam, E., Gani, D., Ryan, M.D.
374 2001. The 'cleavage' activities of foot-and-mouth disease virus 2A site-directed mutants and
375 naturally occurring '2A-like' sequences. J. Gen. Virol. 82:1027-1041.
376 11. Eaton, H.E., Kobayashi, T., Dermody, T.S., Johnston, R.N., Jais, P.H., Shmulevitz, M. 2017.
377 African swine fever virus NP868R capping enzyme promotes reovirus rescue during reverse
378 genetics by promoting reovirus protein expression, virion assembly, and RNA incorporation
379 into infectious virions. J. Virol. 91:e02416-16.
380 12. Eichwald, C., Rodriguez, J.F., Burrone, O.R. 2004. Characterization of rotavirus NSP2/NSP5
381 interactions and the dynamics of viroplasm formation. J. Gen. Virol. 85:625-634.
382 13. Fabbretti, E., Afrikanova, I., Vascotto, F., Burrone, O.R.. 1999. Two non-structural rotavirus
383 proteins, NSP2 and NSP5, form viroplasm-like structures in vivo. J. Gen. Virol. 80:333-339.
384 14. Gault, E., Schnepf, N., Poncet, D., Servant, A., Teran, S., Garbarg-Chenon, A. 2001. A
385 human rotavirus with rearranged genes 7 and 11 encodes a modified NSP3 protein and
386 suggests an additional mechanism for gene rearrangement. J. Virol. 75:7305-7314.
387 15. Gratia, M., Sarot, E., Vende, P., Charpilienne, A., Baron, C.H., Duarte, M., Pyronnet, S.,
388 Poncet, D. 2015. Rotavirus NSP3 is a translational surrogate of the poly(A)-binding protein-
389 poly(A) complex. J. Virol. 89:8773-8782.
390 16. Groft, C.M., Burley, S.K. 2002. Recognition of eIF4G by rotavirus NSP3 reveals a basis for
391 mRNA circularization. Mol. Cell. 9:1273-1283.
392 17. Guglielmi, K.M., McDonald, S.M., Patton, J.T. 2010. Mechanism of intraparticle synthesis
393 of the rotavirus double-stranded RNA genome. J. Biol. Chem. 285:18123-18128.
394 18. Hofacker, I.L. Vienna RNA secondary structure server. 2003. Nucleic Acids Res. 31:3429-
395 3431.

396 19. Hofacker, I.L., Fontana, W., Stadler, P.F., Bonhoeffer, S., Tacker, M., Schuster, P. 1994. Fast
397 folding and comparison of RNA secondary structures. Monatsh. Chemie 125:167–188.
398 20. Imai, M., Akatani, K., Ikegami, N., Furuichi, Y. 1983. Capped and conserved terminal
399 structures in human rotavirus genome double-stranded RNA segments. J. Virol. 47:125–136.
400 21. James, V.L., Lambden, P.R., Deng, Y., Caul, E.O., Clarke, I.N. 1999. Molecular
401 characterization of human group C rotavirus genes 6, 7 and 9. J. Gen. Virol. 80:3181-3187.
402 22. Johne, R., Reetz, J., Kaufer, B.B., Trojnar, E. 2015. Generation of an avian-mammalian
403 rotavirus reassortant by using a helper virus-dependent reverse genetics system. J. Virol.
404 90:1439-1443.
405 23. Kanai, Y., Komoto, S., Kawagishi, T., Nouda, R., Nagasawa, N., Onishi, M., Matsuura, Y.,
406 Taniguchi, K., Kobayashi, T. 2017. Entirely plasmid-based reverse genetics system for
407 rotaviruses. Proc. Natl. Acad. Sci. USA 114:2349-2354.
408 24. Kanai, Y., Kawagishi, T., Nouda, R., Onishi, M., Pannacha, P., Nurdin, J.A., Nomura, K.,
409 Matsuura, Y., Kobayashi, T. 2018. Development of stable rotavirus reporter expression
410 systems. J. Virol. 93: e01774-18.
411 25. Komoto, S., Kanai, Y., Fukuda, S., Kugita, M., Kawagishi, T., Ito, N., Sugiyama, M.,
412 Matsuura, Y., Kobayashi, T., Taniguchi, K. 2017. Reverse genetics system demonstrates that
413 rotavirus nonstructural protein NSP6 is not essential for viral replication in cell culture. J.
414 Virol. 91 pii: e00695-17.
415 26. Komoto, S., Fukuda, S., Ide, T., Ito, N., Sugiyama, M., Yoshikawa, T., Murata, T.,
416 Taniguchi, K. 2018. Generation of recombinant rotaviruses expressing fluorescent proteins
417 by using an optimized reverse genetics system. J. Virol. 92:e00588-18.

418 27. Kumagai, A., Ando, R., Miyatake, H., Greimel, P., Kobayashi, T., Hirabayashi, Y.,
419 Shimogori, T., Miyawaki, A. 2013. A bilirubin-inducible fluorescent protein from eel
420 muscle. Cell 153:1602-1611.
421 28. Kyrieleis, O.J., Chang, J., de la Peña, M., Shuman, S., Cusack, S. 2014. Crystal structure of
422 vaccinia virus mRNA capping enzyme provides insights into the mechanism and evolution of
423 the capping apparatus. Structure 22:452-465.
424 29. Langland, J.O., Pettiford, S., Jiang, B., Jacobs, B.L. 1994. Products of the porcine group C
425 rotavirus NSP3 gene bind specifically to double-stranded RNA and inhibit activation of the
426 interferon induced protein kinase PKR. J. Virol. 68:3821-3829.
427 30. Martínez-Álvarez, L., Piña-Vázquez, C., Zarco, W., Padilla-Noriega, L. 2013. The shift from
428 low to high non-structural protein 1 expression in rotavirus-infected MA-104 cells. Mem.
429 Inst. Oswaldo Cruz. 108:421-428.
430 31. Mohanty, S.K., Donnelly, B., Dupree, P., Lobeck, I., Mowery, S., Meller, J., McNeal, M.,
431 Tiao, G. 2017. A point mutation in the rhesus rotavirus VP4 protein generated through a
432 rotavirus reverse genetics system attenuates biliary atresia in the murine model. J. Virol. 91
433 pii: e00510-17.
434 32. Montero, H., Arias, C.F., Lopez, S. 2006. Rotavirus nonstructural protein NSP3 is not
435 required for viral protein synthesis. J. Virol. 80:9031-9038.
436 33. Navarro, A., Trask, S.D., Patton, J.T. 2013. Generation of genetically stable recombinant
437 rotaviruses containing novel genome rearrangements and heterologous sequences by reverse
438 genetics. J. Virol. 87:6211-6220.
439 34. Patton, J.T., Taraporewala, Z., Chen, D., Chizhikov, V., Jones, M., Elhelu, A., Collins, M.,
440 Kearney, K., Wagner, M., Hoshino, Y., Gouvea, V. 2001. Effect of intragenic rearrangement

441 and changes in the 3' consensus sequence on NSP1 expression and rotavirus replication. J.
442 Virol. 75:2076-2086.
443 35. Rodriguez, E.A., Campbell, R.E., Lin, J.Y., Lin, M.Z., Miyawaki, A., Palmer, A.E., Shu, X.,
444 Zhang, J., Tsien, R.Y. 2017. The growing and glowing toolbox of fluorescent and
445 photoactive proteins. Trends Biochem Sci. 42:111-129.
446 36. Rubio, R.M., Mora, S.I., Romero, P., Arias, C.F., López, S. 2013. Rotavirus prevents the
447 expression of host responses by blocking the nucleocytoplasmic transport ofpolyadenylated
448 mRNAs. J. Virol. 87:6336-6345.
449 37. Salsman, J., Top, D., Boutilier, J., Duncan, R. 2005. Extensive syncytium formation
450 mediated by the reovirus FAST proteins triggers apoptosis-induced membrane instability. J.
451 Virol. 79:8090-8100.
452 38. Settembre, E.C., Chen, J.Z., Dormitzer, P.R., Grigorieff, N., Harrison, S.C. 2011. Atomic
453 model of an infectious rotavirus particle. EMBO J. 30:408–416.
454 39. Shen, S., Burke, B., Desselberger, U. 1994. Rearrangement of the VP6 gene of a group A
455 rotavirus in combination with a point mutation affecting trimer stability. J. Virol. 68:1682-
456 1688.
457 40. Tortorici, M.A., Broering, T.J., Nibert, M.L., Patton, J.T. 2003. Template recognition and
458 formation of initiation complexes by the replicase of a segmented double-stranded RNA
459 virus. J. Biol. Chem. 278:32673-32682.
460 41. Trask, S.D, Taraporewala, Z.F., Boehme, K.W., Dermody, T.S., Patton, J.T. 2010. Dual
461 selection mechanisms drive efficient single-gene reverse genetics for rotavirus. Proc. Natl.
462 Acad. Sci. USA 107:18652-18657.

463 42. Trask, S.D., McDonald, S.M., Patton, J.T. 2012. Structural insights into the coupling of
464 virion assembly and rotavirus replication. Nat. Rev. Microbiol. 10:165–177
465

466 **Figure Legends**

467 **Figure 1.** Wildtype and modified NSP3 proteins encoded by pT7 plasmids and rotaviruses. (A)
468 Organization of pT7 plasmids expressing wild type NSP3 and NSP3-FL/UnaG (+)RNAs,
469 indicating locations of T7 promoter (prm) and Hepatitis delta virus (HDV) self-cleaving
470 ribozyme (Rz). Nucleotide positions are labeled. (B) Products of recombinant RVAs expressing
471 wild type NSP3 and NSP3-FL-UnaG and RVC (Bristol strain) expressing NSP3-2A-dsRBP,
472 including approximate locations of functional domains in NSP3 (Deo et al., 2002; Groft and
473 Burley, 2002). Red arrow indicates the position of the stop-restart cleavage site in the 2A-like
474 element in the RVC NSP3-2A-dsRBP ORF. Amino acid positions are labeled.

475 **Figure 2.** Recovery of recombinant RVA with a modified segment 7 dsRNA that expresses the
476 fused NSP3-FL-UnaG protein. (A) Profiles of the eleven genomic dsRNAs recovered from
477 rSA11 viruses resolved by PAGE. Red arrow notes the position of the segment 7 dsRNA. (B)
478 Western blot analysis of proteins present at 8 h p.i. in MA104 cells infected with recombinant
479 viruses. (C) Plaques produced by recombinant viruses.

480 **Figure 3.** Dimerization of NSP3-FL-UnaG. MA104 cells were mock infected, or infected with
481 rSA11/wt or rSA11/NSP3-FL-UnaG and incubated until 8 h p.i., when cells were harvested. Cell
482 lysates were mixed with sample buffer containing sodium dodecyl sulfate and b-
483 mercaptoethanol, incubated for 10 min either at 25 or 95°C, resolved by electrophoresis on a
484 Novex 8-16% polyacrylamide gel, and the blotted onto a nitrocellulaose membrane. Blots were
485 probed with guinea pig polyclonal anti-NSP3 or anti-VP6 antibodies, or with a mouse anti-
486 PCNA monoclonal antibody. Primary antibodies were detected using horseradish peroxidase-
487 conjugated secondary antibodies. Sizes (kD) of protein markers (M) are indicated. NSP3 band
488 intensities were determined by Image J analysis and were normalized to VP6 band intensities.

489 **Figure 4**. Genetic stability of rRVA/NSP3-FL-UnaG. Virus was serially passaged 5-times in
490 MA104 cells using 1:1000 dilutions of infected cell lysate as inoculum.
491 **Figure 5.** Comparison of UnaG expression by rSA11/NSP3-FL-UnaG versus rSA11/NSP1-FL-
492 UnaG. Images were taken at 24 h p.i. using a Bio-Rad Zoe live-cell imager and similarly
493 processed for presentation.
494 **Figure 6.** pT7 plasmids and rotaviruses expressing NSP1. (A) Organization of pT7 plasmids
495 expressing wild type NSP1 and NSP1-FL-UnaG (+)RNAs, indicating locations of T7 promoter
496 and Hepatitis delta virus self-cleaving ribozymes. The red arrow notes the position of the stop
497 codon in the NSP1-FL-UnaG ORF. (B) Products of recombinant RVAs expressing wild type
498 NSP1 and NSP1-FL-UnaG. (C) Profiles of the eleven genomic dsRNAs recovered from rSA11
499 viruses resolved by PAGE. Red arrow notes the position of the segment 5 dsRNA. (D) Western
500 blot analysis of proteins present at 8 h p.i. in MA104 cells infected with recombinant viruses. (E)
501 Plaques produced by recombinant viruses.
502 **Figure 7.** Conservation of a predicted stable stem-loop structure formed by the 3'-UTR sequence
503 of rSA11/wt and rSA11/NSP3-FL-UnaG. Secondary structures associated with minimum free
504 energy were calculated for segment 7 (+)RNAs using *RNAfold* {http://rna.tbi.univie.ac.at/} and
505 color coded to indicate base-pairing probability (Hokacker, 2003; Hofacker et al., 1994).
506 Portions of the secondary structures are shown that include the 5' and 3' ends of the (+)RNAs
507 (labeled) and the conserved 3' stem-loops (3'SL) (boxed). Also labeled are the start and stop
508 codons (green and red arrowheads, respectively) of both the NSP3 and NSP3-FL-UnaG ORFs.
509 **Figure S1.** Influence of plasmids on the recovery of recombinant RVAs. In two independent RG
510 experiments, BHK-T7 cells were co-transfected with mixtures of pT7 SA11 plasmids that
511 contained pT7/NSP3-3xFL-UnaG in place of pT7/NSP3SA11. As indicated, some plasmid

512 mixtures included pCMV/NP868R and/or 3x levels of pT7 NSP2SA11 and NSP5SA11
513 plasmids. After 2 days, transfected BHK-T7 cells were overseeded with MA104 cells. Titers of
514 viruses in lysates prepared from the MA104/BHK-T7 cells at 5 days p.i. were determined by
515 plaque assay. Each RG experiment was performed with a separately prepared set of plasmids,
516 and plaque assays were performed in duplicate.
517

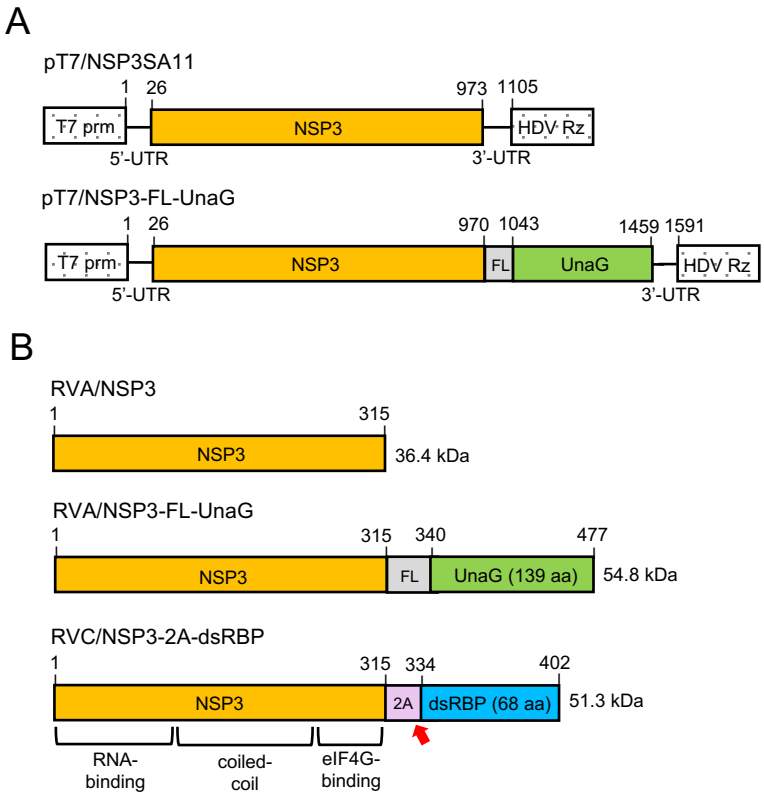

Figure 1. Wildtype and modified NSP3 proteins encoded by pT7 plasmids and rotaviruses. (A) Organization of pT7 plasmids expressing wild type NSP3 and NSP3-FL/UnaG (+)RNAs, indicating locations of T7 promoter (prm) and Hepatitis delta virus (HDV) self-cleaving ribozyme (Rz). Nucleotide positions are labeled. (B) Products of recombinant RVAs expressing wild type NSP3 and NSP3-FL-UnaG and RVC (Bristol strain) expressing NSP3-2A-dsRBP, including approximate locations of functional domains in NSP3 (Deo et al., 2002; Groft and Burley, 2002). Red arrow indicates the position of the stop-restart cleavage site in the 2A-like element in the RVC NSP3-2A-dsRBP ORF. Amino acid positions are labeled.

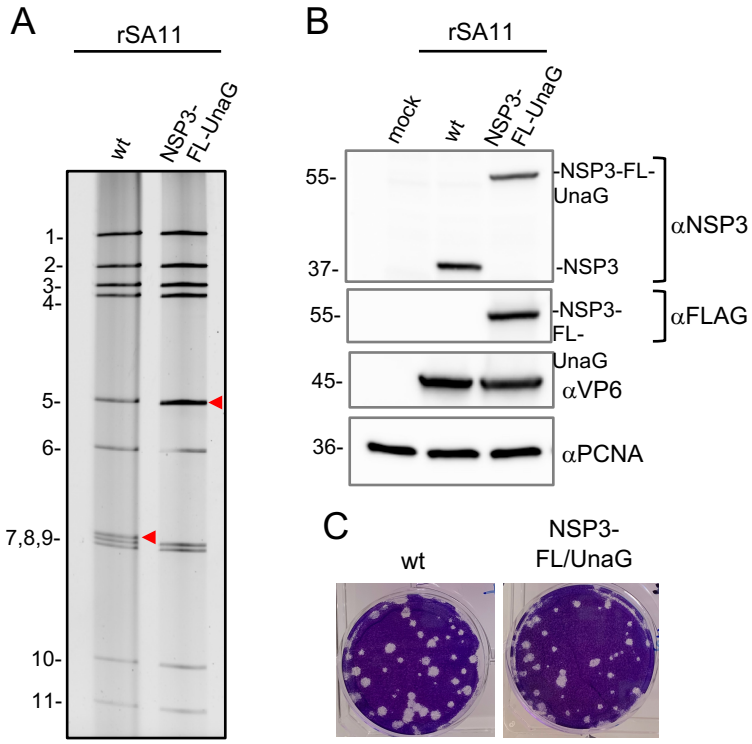

Figure 2. Recovery of recombinant RVA with a modified segment 7 dsRNA that expresses the fused NSP3-FL-UnaG protein. (A) Profiles of the eleven genomic dsRNAs recovered from rSA11 viruses resolved by PAGE. Red arrow notes the position of the segment 7 dsRNA. (B) Western blot analysis of proteins present at 8 h p.i. in MA104 cells infected with recombinant viruses. (C) Plaques produced by recombinant viruses.

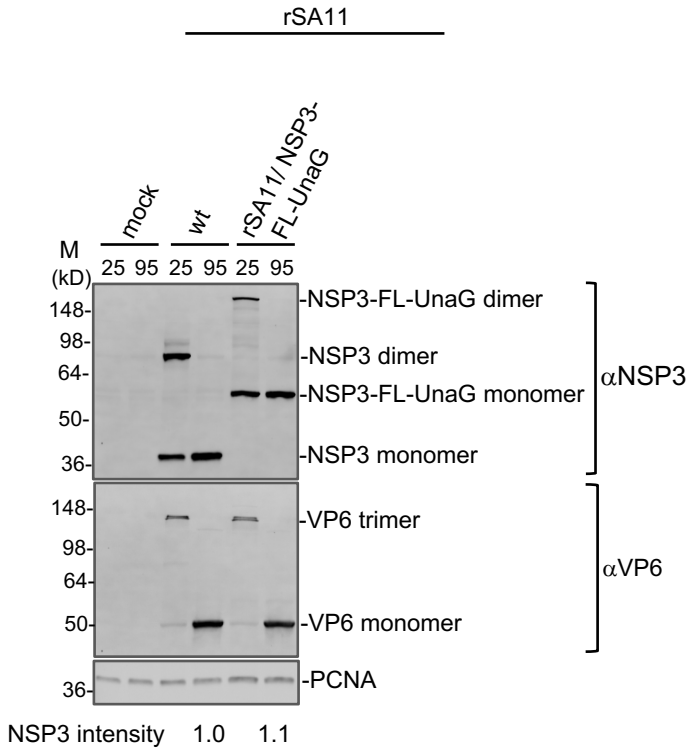

Figure 3. Dimerization of NSP3-FL-UnaG. MA104 cells were mock infected, or infected with rSA11/wt or rSA11/NSP3-FL-UnaG and incubated until 8 h p.i., when cells were harvested. Cell lysates were mixed with sample buffer containing sodium dodecyl sulfate and β-mercaptoethanol, incubated for 10 min either at 25 or 95ºC, resolved by electrophoresis on a Novex 8-16% polyacrylamide gel, and the blotted onto a nitrocellulaose membrane. Blots were probed with guinea pig polyclonal anti-NSP3 or anti-VP6 antibodies, or with a mouse anti-PCNA monoclonal antibody. Primary antibodies were detected using horseradish peroxidase-conjugated secondary antibodies. Sizes (kD) of protein markers (M) are indicated. NSP3 band intensities were determined by Image J analysis and were normalized to VP6 band intensities.

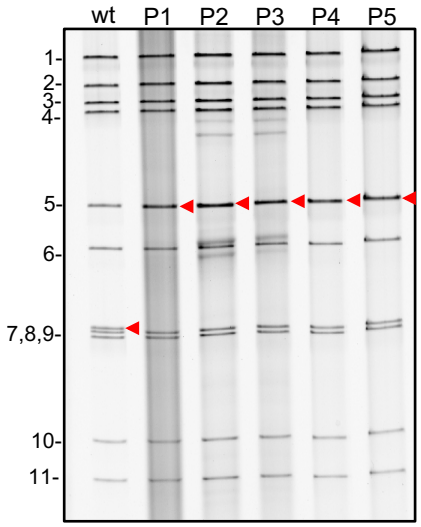

Figure 4. Genetic stability of rRVA/NSP3-FL-UnaG. Virus was serially passaged 5-times in MA104 cells using 1:1000 dilutions of infected cell lysate as inoculum.

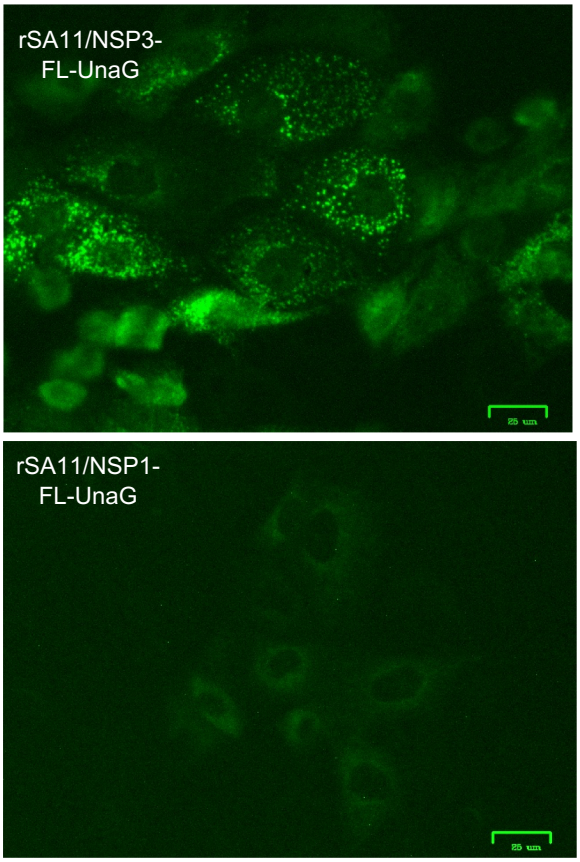

Figure 5. Comparison of UnaG expression by rSA11/NSP3-FL-UnaG versus rSA11/NSP1-FL-UnaG. Images were taken at 24 h p.i. using a Bio-Rad Zoe live-cell imager and similarly processed for presentation.

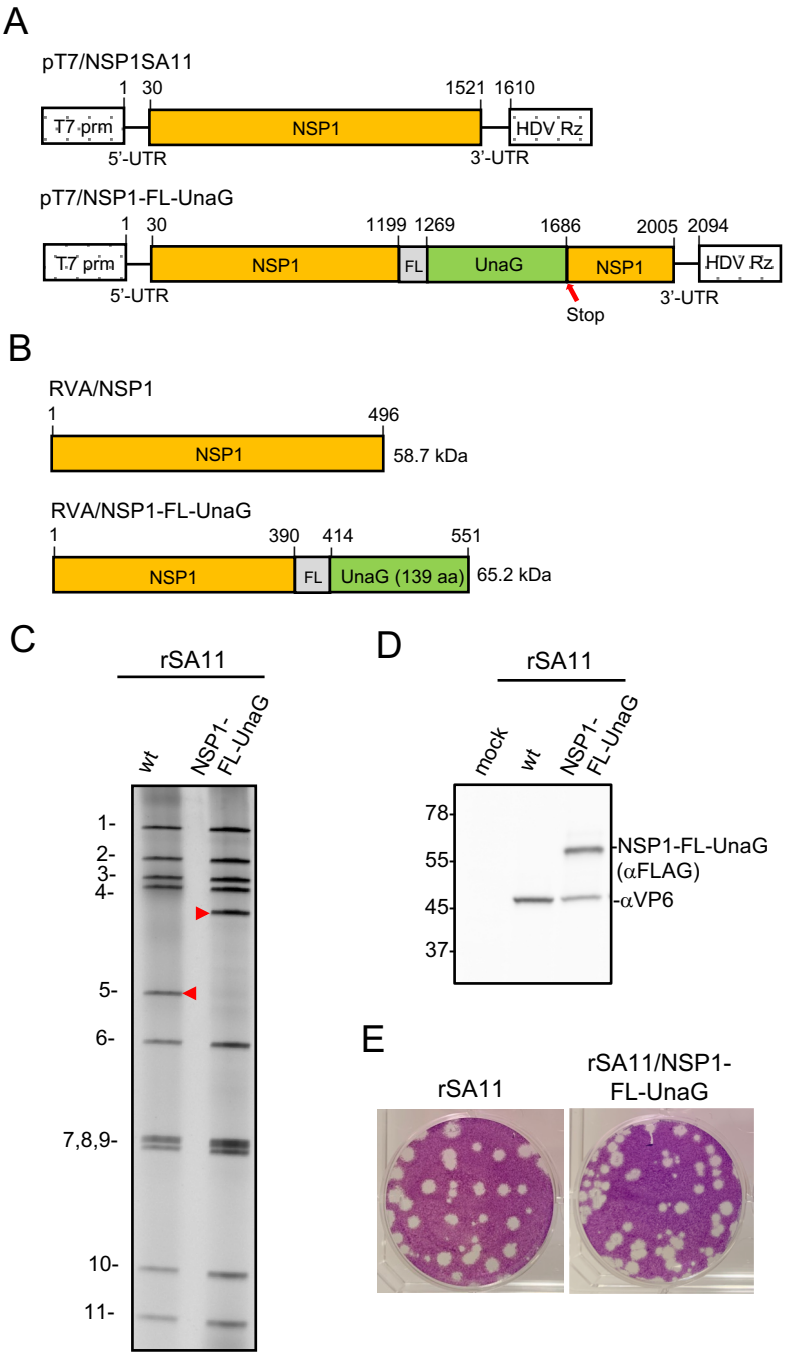

Figure 6. pT7 plasmids and rotaviruses expressing NSP1. (A) Organization of pT7 plasmids expressing wild type NSP1 and NSP1-FL-UnaG (+)RNAs, indicating locations of T7 promoter and Hepatitis delta virus self-cleaving ribozymes. The red arrow notes the position of the stop codon in the NSP1-FL-UnaG ORF. (B) Products of recombinant RVAs expressing wild type NSP1 and NSP1-FL-UnaG. (C) Profiles of the eleven genomic dsRNAs recovered from rSA11 viruses resolved by PAGE. Red arrow notes the position of the segment 5 dsRNA. (D) Western blot analysis of proteins present at 8 h p.i. in MA104 cells infected with recombinant viruses. (E) Plaques produced by recombinant viruses.

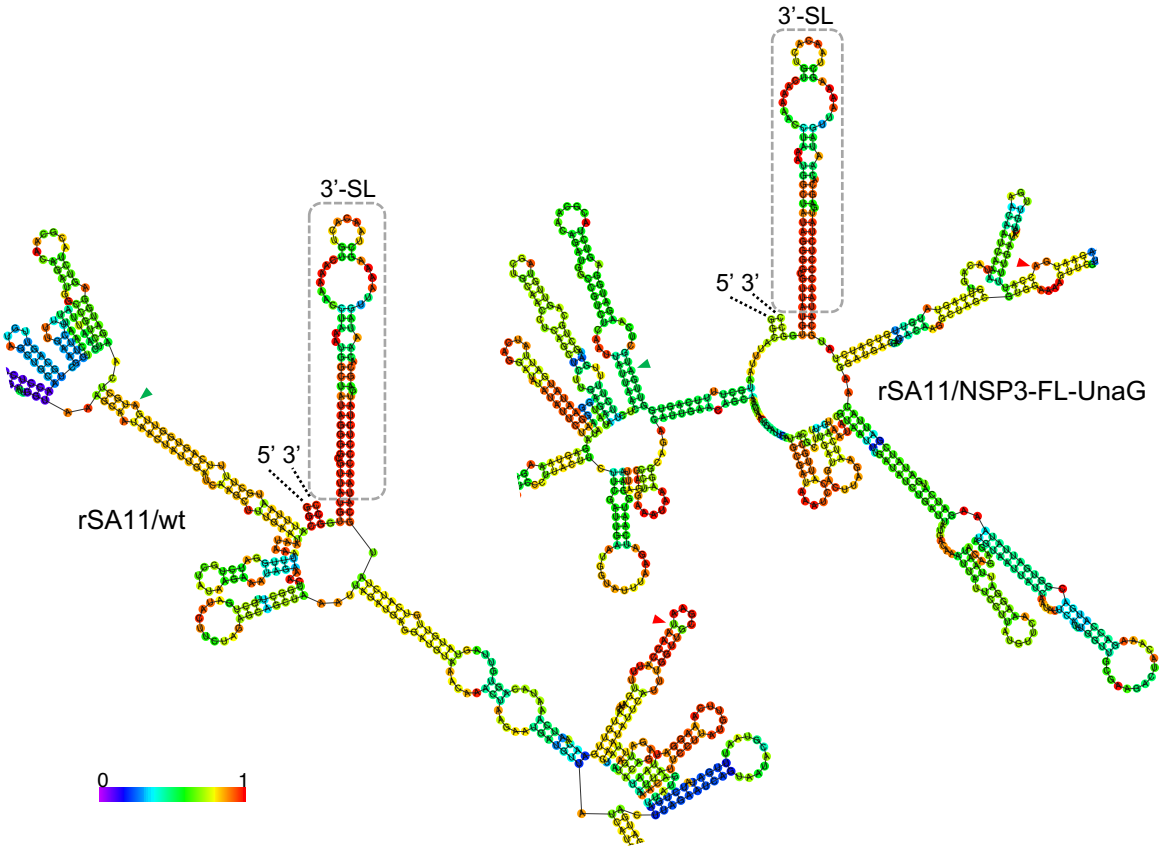

Figure 7. Conservation of a predicted stable stem-loop structure formed by the 3'-UTR sequence of rSA11/wt and rSA11/NSP3-FL-UnaG. Secondary structures associated with minimum free energy were calculated for segment 7 (+)RNAs using *RNAfold* {http://rna.tbi.univie.ac.at/} and color coded to indicate base-pairing probability (Hokacker, 2003; Hofacker et al., 1994). Portions of the secondary structures are shown that include the 5' and 3' ends of the (+)RNAs (labeled) and the conserved 3' stem-loops (3'SL) (boxed). Also labeled are the start and stop codons (green and red arrowheads, respectively) of both the NSP3 and NSP3-FL-UnaG ORFs.